

Online Research @ Cardiff

This is an Open Access document downloaded from ORCA, Cardiff University's institutional repository: <https://orca.cardiff.ac.uk/id/eprint/105953/>

This is the author's version of a work that was submitted to / accepted for publication.

Citation for final published version:

Sapsford, Devin James ORCID: <https://orcid.org/0000-0002-6763-7909> and Tufvesson, S. 2017. Properties of recycled sludge formed from different aluminiferous reagents during the ettringite process. Journal of Water Process Engineering 19 , pp. 305-311. 10.1016/j.jwpe.2017.08.016 file

Publishers page: <http://dx.doi.org/10.1016/j.jwpe.2017.08.016>
<<http://dx.doi.org/10.1016/j.jwpe.2017.08.016>>

Please note:

Changes made as a result of publishing processes such as copy-editing, formatting and page numbers may not be reflected in this version. For the definitive version of this publication, please refer to the published source. You are advised to consult the publisher's version if you wish to cite this paper.

This version is being made available in accordance with publisher policies.

See

<http://orca.cf.ac.uk/policies.html> for usage policies. Copyright and moral rights for publications made available in ORCA are retained by the copyright holders.



Properties of recycled sludge formed from different aluminiferous reagents during the ettringite process

D.J. Sapsford, S. Tufvesson

Cardiff School of Engineering, Cardiff University, Cardiff, CF24 3AA, UK

Abstract

Development of processes for the removal of sulfate ions from mine waters and industrial effluents is ongoing. A number of processes involve the removal of sulfate as ettringite, a calcium aluminum sulfate ($\text{Ca}_6\text{Al}_2(\text{SO}_4)_3(\text{OH})_{12}\cdot 26\text{H}_2\text{O}$) at elevated pH (11.5–13). Various process configurations have been proposed using lime in combination with an aluminiferous reagent to react with the sulfate in the effluent. This paper presents a study of the effect of the source of aluminum (when mixed with lime and synthetic sodium sulfate-rich effluent) on the physicochemical properties of the resultant ettringite sludge and on the propensity of the precipitate, when recycled, to form high density sludge (HDS). It is demonstrated that aluminum chloride, aluminum nitrate and polyaluminum chloride all remove sulfate as ettringite, with aluminum chloride removing sulfate to the lowest residual concentration. Sodium aluminate proved least effective at removal of sulfate for >1 cycle, and early process cycles produced a precipitate that may have been a mixture of minerals including ettringite and calcium aluminate monosulfate. Laboratory synthesised aluminum hydroxide and crystalline gibbsite were unreactive to sulfate. The different aluminiferous reagents influenced the resultant sludge volume and sludge settling velocity, with sodium aluminate forming a relatively voluminous sludge with low settling velocity and aluminum chloride-derived ettringite forming the densest 'single-pass' sludge and consistently the fastest settling sludge. Recycling of sludge in the process seemingly improves the precipitation kinetics, with lower residual sulfate concentrations found for the same reaction time upon sludge recycling. All sludges showed a slight propensity to form HDS upon recirculation. Microscope images show differences in the precipitate morphology between different aluminiferous reagents and upon recycling of sludge, typically there was an evolution from small spherical precipitates to increasing amounts of needle-shaped crystals upon recycling. These results highlight the importance of understanding how the choice of aluminiferous reagent influences the micro- and macroscopic properties of the resultant sludge, with the commensurate implications this has for process design when applying the ettringite precipitation process for the removal of sulfate from effluents.

1. Introduction

Elevated concentrations of the sulfate ion ($\text{SO}_4^{2-}(\text{aq})$) occur in a range of mining and industrial effluents including mine drainage; mineral slurry transport water; effluents from smelting operations; hydraulic fracturing flow back; effluents from the manufacture of paper, textiles, fertilisers, dyes, glass, soaps, fungicides, and tanneries [1,2]; and root crop processing e.g. ginger and beet and aluminum anodising [3].

Sulfate is not regarded as toxic to humans at the levels typically encountered in the environment. However, sulfate is regarded as an aesthetic pollutant in drinking water with the taste threshold generally lying between 250 mg/L and 1000 mg/L for sodium and calcium sulfate respectively. The World Health Organisation (WHO) recommends a 250 mg/L threshold [4]. Waters and effluents containing in excess of 500 mg/L sulfate are considered potentially hazardous to concrete [5] affecting infrastructure such as sewers through damage caused by the formation of secondary ettringite. In recent years environmental regulators have become more concerned with high sulfate concentrations in effluents and different countries have adopted a range of approaches to regulating sulfate with many setting specific sulfate limits. Sulfate is also

indirectly a target of regulation through tightening of Total Dissolved Solids (TDS) limits in many jurisdictions where sulfate comprises a key contributor to the elevated TDS [6].

Removal technologies for sulfate from sulfate-rich effluents have been reviewed (e.g. [7,6] and include (i) chemical addition to induce the precipitation of insoluble/sparingly-soluble sulfate salts including gypsum, ettringite (e.g. [8]; barium sulfate (e.g. [9,10] and jarosite (e.g. [11]; (ii) removal using membrane processes such as electrodialysis, reverse osmosis and nanofiltration (iii) ion exchange (iv) biological treatment utilising microbiological sulfate reducing organisms, and (v) evaporation/crystallisation. It is noteworthy that membrane processes comprise only partial treatment in that a reject sulfate brine is produced which will require chemical precipitation or evaporative crystallisation to produce a solid for final disposal. With respect to the chemical precipitation processes, ettringite precipitation processes are considered particularly promising [6]. The reaction occurs at elevated pH (11.5–13) and involves reaction of dissolved sulfate with aluminum and calcium reagents such that ettringite ($\text{Ca}_6\text{Al}_2(\text{SO}_4)_3(\text{OH})_{12}\cdot 26\text{H}_2\text{O}$) precipitates. This paper concerns the composition, morphology, and mineralogy of precipitates that form during the ettringite process for the removal of sulfate.

The term ettringite is used to refer to both the mineral and the ettringite crystal structure [12,13]. Parallel columns comprising Ca^{2+} , Al^{3+} and OH^- -structured units of $[\text{Ca}_6\text{Al}_2(\text{OH})_{12}\cdot 24\text{H}_2\text{O}]^{6+}$ are characteristic of the ettringite crystal structure. Water and sulfate ions exist within channels formed between the structural columns which balance out the structural charge [14,13]. The mineral can exchange some of its ions without adverse structural change [13] and the water content can be variable with between 24 and 32 moles of water per mole of ettringite but this does not impact the XRD response upon analyses [12].

Most literature regarding ettringite comes from the field of concrete technology and waste stabilisation (e.g. [15]) as ettringite is a common constituent phase important in developing early stage strength and also causes problematic secondary or delayed ettringite formation. Consequently, literature on physicochemical and morphological aspects of ettringite relevant to this study focuses on much slower processes in concrete rather than the short residence times within water treatment processes. Nevertheless, there are several useful insights – Cody et al. [16] investigated how the nucleation and growth of the ettringite crystals were affected by different chemicals and demonstrated that different precipitate morphologies result from the presence of a range of additives and their concentration.

With respect to the literature on ettringite during sulfate removal processes for effluent treatment, there are only a small number of publications covering the effectiveness of different reagents in removing sulfate as ettringite (e.g. Janneck et al. [17]) and there is an absence of studies looking at the influence of aluminiferous reagent and sludge recycling on the physicochemical properties of the resultant sludge. This study came about after preliminary trials of an ettringite precipitation process indicated problematic volumes of precipitate. Similar problems with voluminous ‘single-pass’ sludge has commonly experienced with metal precipitation from mine waters and industrial effluents with typical sludges having a solids contents of only 1–5%. The High Density Sludge (HDS) process was developed in response to this problem [18,19]. Process sludge is recycled from the clarifier to the reactor tanks leading to densification of the sludge to solids concentrations of 15–35%, improved settling velocities, dewaterability and reduced resistance to filtration which equates to better process economics [20]. It was noted that some of the current proprietary ettringite precipitation processes involve sludge recycling. Thus the aims of this study were to (i) ascertain the properties of single pass sludge for different aluminiferous reagents, and (ii) to determine how residual sulfate, settling rates, sludge volume, morphology, chemical composition and mineralogy vary when recycling sludge using different aluminiferous reagents.

2. Materials and methods

The experiments were carried out as bench scale batch tests and adapted from the HDS experiments of Bosman [21]. The experiments involved treatment of a sodium sulfate feed by addition of stoichiometric quantities of aluminiferous reagent and a 10% stoichiometric excess of lime. The feed was limited to $[\text{SO}_4^{2-}] = 1500 \text{ mg/L}$ to avoid precipitation of gypsum. The reagents were used in solution or slurry form prepared in deionized water and of the following strengths (% w/v): sodium sulfate (Na_2SO_4) – 2.22% solution; calcium hydroxide ($\text{Ca}(\text{OH})_2$) – 5% slurry (kept suspended using a magnetic stirrer). Aluminiferous reagents used were as follows: aluminum chloride ($\text{AlCl}_3\cdot 6\text{H}_2\text{O}$) – 25% solution; sodium aluminate – 8.5% NaAlO_2 solution; polyaluminum chloride (PAC) – 10% solution; aluminum nonahydrate ($\text{Al}(\text{NO}_3)_3\cdot 9\text{H}_2\text{O}$) – 22%; aluminum hydroxide ($\text{Al}(\text{OH})_3$) powder; and synthesised aluminum hydroxide. The synthesised aluminum hydroxide was produced by neutralising 250 ml of a 2% AlCl_3 solution with NaOH . This resulted in a gel which was filtered, rinsed thoroughly with deionized water and dried at 105 °C for 48 h.

The batch tests were conducted either as ‘single pass’ or as ‘recycled’ as follows: 100 ml ($\pm 1 \text{ ml}$) of the Na_2SO_4 feed solution was added to a beaker placed on a magnetic stirrer. Reactions were started by introduction of 4 ml of the $\text{Ca}(\text{OH})_2$ slurry. This was followed by addition of aluminiferous reagent. Immediately afterwards an additional 1.1 ml $\text{Ca}(\text{OH})_2$ was added. The suspension was stirred for 15 min and pH recorded. The suspension was transferred to a volumetric measuring cylinder and the sludge allowed to settle for 15 min. A 15 min settling period (rather than 30 min typically used in similar studies) was found to achieve acceptable liquid/solid separation and was used throughout the experimentation, this made experiments with multiple repeat cycles more practicable. During the 15 min the volume of settled sludge and the distance the sludge had settled were continuously recorded to allow the settling velocity to be calculated. This was the end point for ‘single pass’ experiments.

For all non-final cycle (i.e. where the sludge was to be recycled) experiments, at the end of settling the supernatant was carefully decanted off and the sludge returned to the reaction beaker. 100 ml of Na_2SO_4 feed solution was added to the sludge in the reaction beaker and the next cycle begun. The experiments were thereafter repeated according to this procedure for between 1 and 6 cycles for NaAlO_2 , PAC and $\text{Al}(\text{NO}_3)_3\cdot 9\text{H}_2\text{O}$. Because of the promising performance of AlCl_3 , this reagent was used for 12 cycles. The aluminum hydroxide powder was only taken through 1–3 cycles and thereafter discontinued.

To obtain images of the precipitate morphology 0.5 ml of suspension was removed during the 14th minute of the final cycle for recycled sludge experiments. The sample was spread across a petri dish and immediately oven dried at 35 °C for 24 h prior to imaging under an

optical microscope. At the end of all experiments solids were recovered by filtration, oven dried at 35 °C (for 24 h) and weighed. The dry samples were analyzed by X-Ray Diffraction (XRD) performed using a Phillips Philips PW1710 Xpert Pro diffractometer with a CoKa radiation source (generator voltage of 40 keV; tube current of 30 mA). Spectra were acquired between 2 θ angles of 5–90°, with a step size of 0.02° and a 2 s dwell time. Following the XRD analysis the dried samples were acid digested and analyzed using the Perkin Elmer Optima 2100 DV Inductively Coupled Plasma Optical Emission Spectrometer (ICP-OES) for Ca, S and Al.

3. Results and Discussion

3.1. Effectiveness of aluminum hydroxide as an aluminiferous reagent

For the single pass experiments significant sulfate removal was only observed with AlCl_3 , NaAlO_2 , PAC and $\text{Al}(\text{NO}_3)_3$. The XRD and ICP-OES results for both the powdered and the laboratory synthesised aluminum hydroxide showed virtually no sulfate removal and no sign of ettringite being formed. Attempts of recycling did not change these results and it was deemed that aluminum hydroxide in these forms was not able to react to produce ettringite. This is in agreement with the findings of Janneck et al. [17] who found that none of the three crystalline $\text{Al}(\text{OH})_3$ -based reagents were able to substantially reduce sulfate concentrations, attributed to the reagent not being “active”. Despite this, other authors have described $\text{Al}(\text{OH})_3$ being used as reagent in sulfate removal (e.g. [25] albeit with longer reported reaction times of 30–300 min. [26] report the use of “amorphous” $\text{Al}(\text{OH})_3$ at a dose of 0.784 g/L which reduced sulfate concentrations from 1043 ppm to 213 ppm in 15 min.

3.2. Final recorded pH after reaction

Following the mixing of the Na_2SO_4 feed, $\text{Ca}(\text{OH})_2$ slurry and the aluminum source (AlCl_3 , NaAlO_2 , PAC or $\text{Al}(\text{NO}_3)_3$) it was observed through changes in pH that reaction was occurring instantaneously for all other aluminiferous reagents used. The AlCl_3 , PAC and $\text{Al}(\text{NO}_3)_3$ were acidic solutions which resulted in a slightly lower pH of the reacting solution (however still within pH range required for ettringite formation) compared to that generated from the alkaline NaAlO_2 solution. Table 1 gives the ranges of pH measured for single pass and recycled sludge reacting mixtures.

3.3. Residual sulfate concentrations and sludge volumes from the single pass process

After a 15 min ‘single pass’ reaction it was found that AlCl_3 , $\text{Al}(\text{NO}_3)_3$ and PAC all reduced sulfate concentration to less than 300 mg/L. There were considerable

variability in sulfate removal between the single pass repeats for AlCl_3 , $\text{Al}(\text{NO}_3)_3$ and PAC and only AlCl_3 achieved an average residual sulfate concentrations of less than 250 mg/L (the WHO taste threshold). Furthermore, AlCl_3 resulted in a smaller sludge volume (16 ml) than all other reagents, particularly compared to NaAlO_2 which for a poorer residual sulfate (525 mg/L) consistently produced five times the volume of sludge (80 ml). Fig. 1 shows the variations in residual sulfate concentrations and volume of sludge produced. Other literature do not report sludge volumes, but show variable residual sulfate concentrations depending on reagent dose and reaction time. For example very low residual concentrations of sulfate of between 6 and 15 mg/L using PAC or NaAlO_2 -based reagents and 20 mg/L using AlCl_3 were found by Janneck et al. [17] and [27] respectively but at higher doses than used here and longer reaction times of 1–2 h.

3.4. Effect of sludge recycling on residual sulfate concentrations and sludge volumes

When sludge was recycled it was found that the sulfate concentration in the supernatant after recycling (Fig. 2) were reduced to less than 250 mg/L for AlCl_3 , $\text{Al}(\text{NO}_3)_3$ and PAC. This was apparent after just one round of recycling and this behaviour continued upon further recycling. This suggests that the presence of recycled solids improved precipitation kinetics compared with the homogenous single pass system. Recycling of NaAlO_2 leads to a decrease in sulfate concentration but it should be noted that there is significant dilution due to recycling of water entrained within the voluminous sludge.

A clear indicator for the formation of higher density sludge is if the cumulative volume of sludge is non-linear with increased number of cycles i.e. each additional cycle appears to add less sludge than previous cycles. Fig. 3 presents the sludge volume predicted to form without sludge densification versus the actual measured volumes upon recycling. The predicted volumes were calculated by using the first cycle volume to sulfate removal relationship and calculating the volume of new sludge each cycle should produce based on the observed sulfate removal and this relationship (also taking into account dilution by water entrained within recycled sludge). For NaAlO_2 the resultant sludge densified during recycling reaching 76% of the projected volume after 6 cycles. The AlCl_3 -derived sludge slightly densifies over the course of 5–7 cycle reaching a maximum density of 65% of the expected volume at Cycle 8, the densification apparently ceases after 10 cycles. Similarly $\text{Al}(\text{NO}_3)_3$ densified, decreasing to 64% of the expected volume after 4 cycles before returning to expected volume by Cycle 6. PAC derived sludge densified achieving 65% of the expected volume after 5 cycles.

Table 1. pH after 15 min for single pass and recycled sludge mixtures.

	pH	
	Single pass (# replicates)	Cycles 1-6
AlCl_3	11.4-11.8 (3)	11.3-11.9
NaAlO_2	12.4-12.6 (3)	12.3-12.7
$\text{Al}(\text{NO}_3)_3$	11.4-11.7 (2)	11.3-11.7
PAC	11.6-12.1 (3)	11.6-12.2

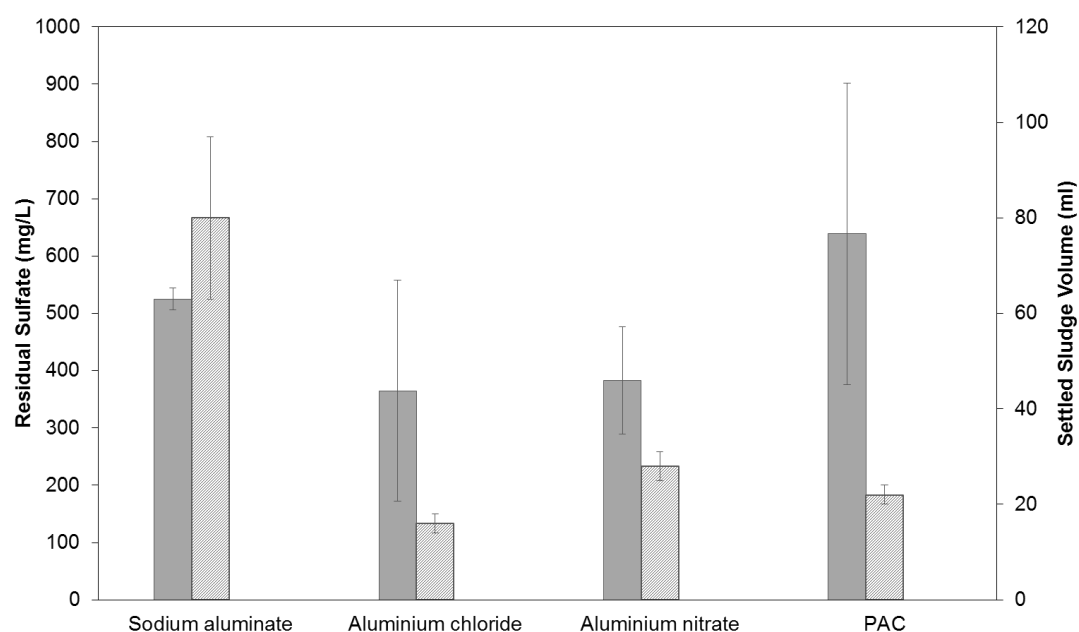


Fig 1. Average residual sulfate concentration (left hand bars/axis) and settled sludge volume (right hand bars/axis) for single pass experiments (error bars represent \pm stdv).

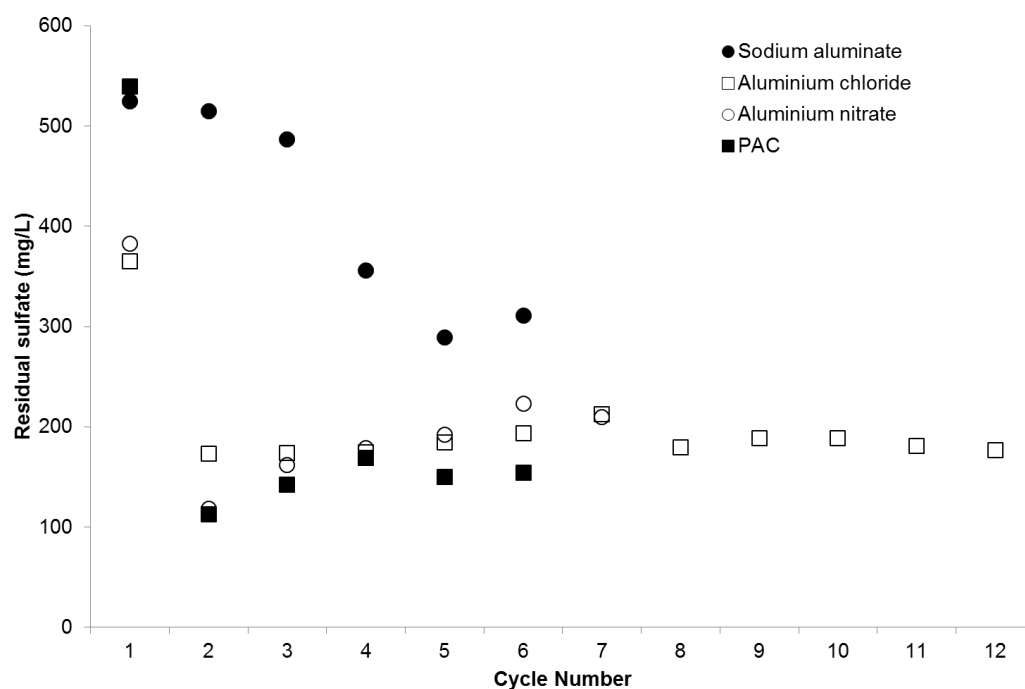


Fig 2. Residual sulfate concentration in supernatants with sludge recycling

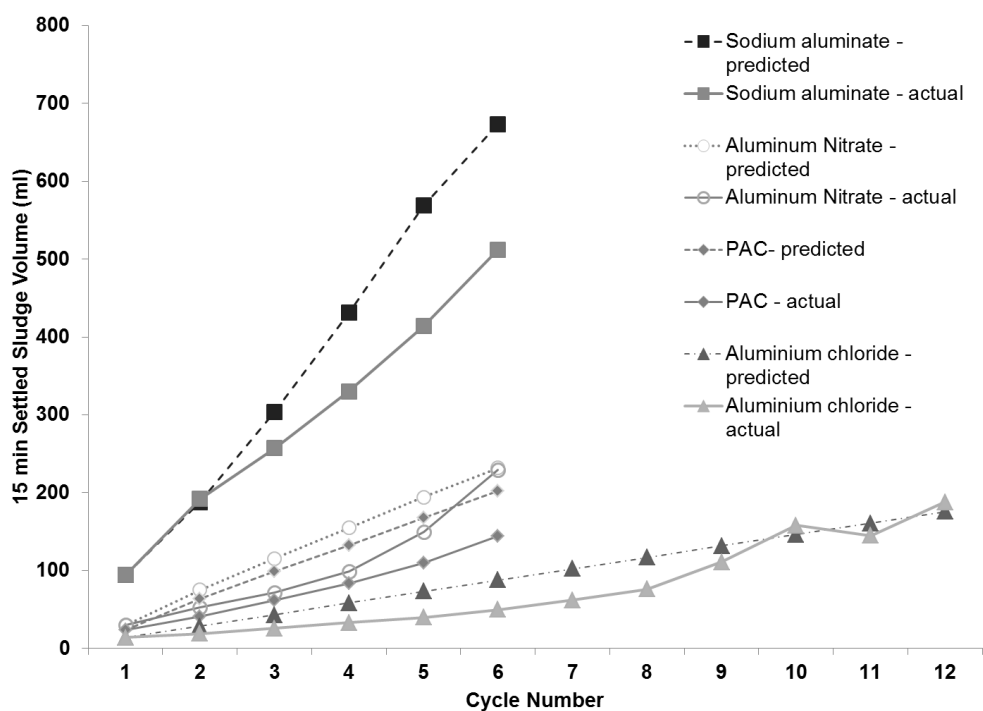


Fig 3. Settled sludge and predicted sludge volumes after 15 min of settling with sludge recycling

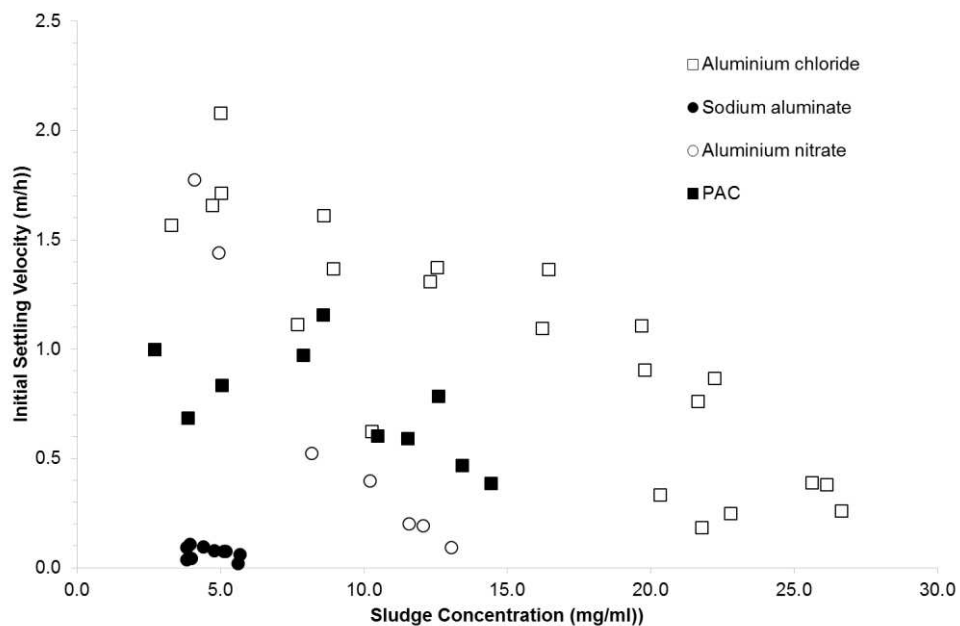


Fig 4. Initial settling velocity versus ettringite slurry concentration.

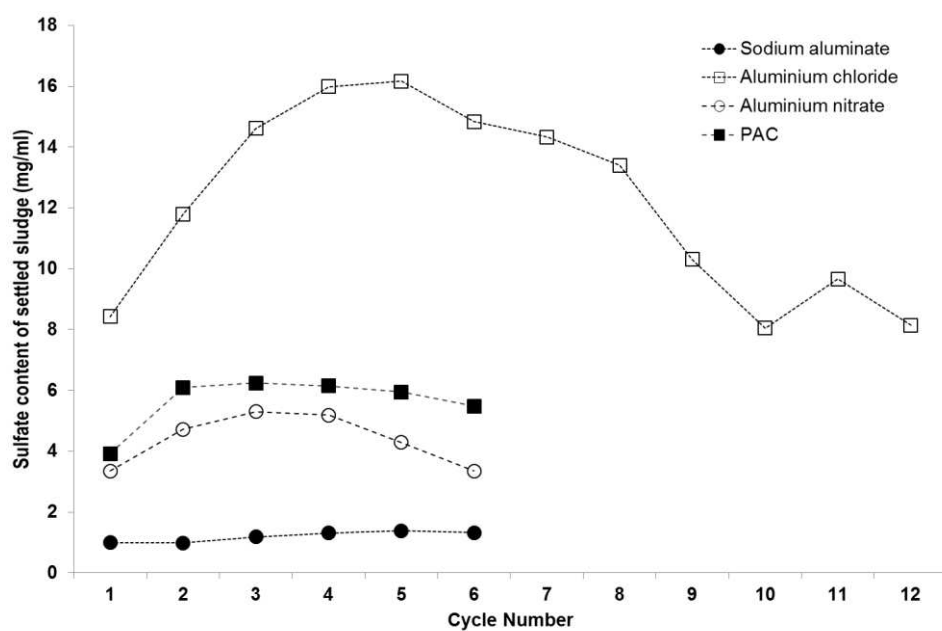


Fig 5. Calculated sulfate bound per unit volume of sludge after 15 min of settling.

The initial settling velocity determined for the sludge solids was found, as expected, to decrease with increased solid concentration for all reagents (Fig. 4). It can be seen that the NaAlO_2 -derived sludge had a much lower settling velocity than AlCl_3 -derived sludge across all solids concentrations. For the first cycle (lowest solids concentrations) the relative initial settling velocities were $\text{AlCl}_3 > \text{Al}(\text{NO}_3)_3 > \text{PAC} > \text{NaAlO}_2$. But as solid concentrations increased (as sludge was recycled) the $\text{Al}(\text{NO}_3)_3$ -derived sludge becoming much slower settling and behaved similarly to the NaAlO_2 -derived sludge.

Fig. 5 shows the sulfate concentration in the sludge (mg/ml) and takes into account the dilution of sulfate caused by recycling of entrained water with recycled sludge. As can be seen in Fig. 5, the AlCl_3 -derived sludge has by far the highest sulfate content and this peaks between the 4th and 5th cycle, decreasing thereafter. $\text{Al}(\text{NO}_3)_3$ and PAC sludge sulfate content peaks between the 3rd to 4th cycle, while the sulfate content of the NaAlO_2 -derived sludge does not change with increased number of cycles.

3.5. Precipitate composition, morphology and mineralogy

The digestion and analyses of the final cycle sludge allowed elemental composition to be determined and demonstrated whether elemental ratios of Al, Ca and S were indicative of ettringite formation (where $\text{Al}:\text{Ca}:\text{S} = 1:4.46:1.78$), the results are shown in Fig. 6 presented normalised to unit aluminum mass. The theoretical ettringite bars refers to the mass proportions of ettringite in the form of $\text{Ca}_6\text{Al}_2(\text{SO}_4)_3(\text{OH})_{12} \cdot 26\text{H}_2\text{O}$. The solids formed from AlCl_3 , $\text{Al}(\text{NO}_3)_3$ and PAC (3 and 6 cycle) show relative proportions of Al, S and Ca consistent with the composition of ettringite. The slight, but consistent larger mass of Ca is believed to have come from either unreacted lime or small amounts of calcite. NaAlO_2 does not conform to ideal ettringite formula until the 6th cycle. Another possible mineral phase in the system is calcium aluminate monosulfate – $3\text{CaO} \cdot \text{Al}_2\text{O}_3 \cdot \text{CaSO}_4 \cdot 12\text{H}_2\text{O}$ [16,22]. The ratio of $\text{Al}:\text{Ca}:\text{S}$ is 1:2.97:0.59 in the monosulfate mineral, the lower proportions of Ca and S relative to Al observed at early times in the NaAlO_2 system (and possibly PAC cycle 1) may be indicative of a mixture of ettringite and calcium aluminate monosulfate having formed. However, the exact ratios observed could not be recreated using a combination of the ettringite and monosulfate as end-members. For example the ratio of $\text{Al}:\text{Ca}:\text{S}$ was 1:3.87:0.96 for NaAlO_2 cycle 1 (single pass) sludge and this in theory could be formed by a mixture of 31% ettringite and 69% monosulfate but the calculated Ca ratio to Al is 3.43 rather than the measured 3.87. Similarly, a mixture of 5.5% ettringite and 94.5% monosulfate would yield a ratio of $\text{Al}:\text{Ca}:\text{S}$ of 1:3.05:0.66, matching the Al and S ratio for the 3rd cycle NaAlO_2 but again underpredicting the amount of Ca observed in the solid, although this could be related to a small amount of residual lime or presence of CaCO_3 . It is however clear that for 1 and 3 cycles the NaAlO_2 does not produce pure

ettringite as the other reagents have, but after 6 cycles elemental ratio suggest pure ettringite dominates the composition.

Observations of crystal morphology (following Cody et al. [16]) were made during examination of the precipitates under optical microscope and are recorded in Table 2. In the cycle 1 (single pass) all precipitates comprised same small round crystallites ($\sim 1 \mu\text{m}$) although aluminum chloride and nitrate also had occasional needles. Generally, as the precipitates were recycled the morphology tended towards and increase in the abundance of needle-like crystals, and clumps/aggregates of crystallites with radiating edges (see for example Fig. 7(b) and (d)). However, precipitates from using sodium aluminate had the least development of this secondary needle-like morphology after 6 cycles. The morphology and crystal size for precipitates from some aluminiferous reagents is very different upon recycling as can be clearly by comparing the images of the precipitates between Fig. 7(a) and (b) and (c) and (d) and the observations noted in Table 2.

Comparison of XRD spectra for different aluminiferous reagent and for cycle number are shown in Fig. 8. It is clear that for AlCl_3 , $\text{Al}(\text{NO}_3)_3$ and PAC that strong clear spectra are generated from all precipitates. All these spectra are characteristic of ettringite but interestingly, the compositional differences detected (Fig. 6) for sodium aluminate are reflected in the weaker XRD response (Fig. 8 (a)), note that this is not simply related to crystallite size as this does not change for cycle 1 and 3 but the XRD spectra do. Although ettringite was identified as the mineral phase, the precipitate is clearly less crystalline but becomes more crystalline by the 6th cycle. This is concurrent with evolution to an ettringite composition (Fig. 6) and the appearance of needle-shaped crystals in the microscope images of the precipitate (Table 2).

It is noteworthy that the XRD response in all cases can be seen to get stronger as the more precipitates are recycled, this can most clearly be seen over the 12 cycles for aluminum chloride (Fig. 8 (b)). These morphological and mineralogical differences are comparable with findings from Cody et al. [16] who reported significant differences in the morphology and minerals formed depending on varying additives participating in the reaction. The chemical environment in which ettringite (or related minerals) precipitate seemingly does not only affect the crystals on a microscopic scale but also on a macroscopic scale in terms of the behaviour and properties of the sludge. Given that ettringite readily exchanges anions such as $\text{B}(\text{OH})_4^-$, SeO_4^{2-} , CrO_4^{2-} and MoO_4^{2-} [23] then real effluents may have a profound affect on the properties of the sludge. In addition other poisoning of the crystal structure during growth may have similar effects: calcium can be replaced by Pb and Sr [24], Al by Cr, Si, Ti, Co, Mn, Fe, Ga, and Ge (see Cody et al. [16] and references therein).

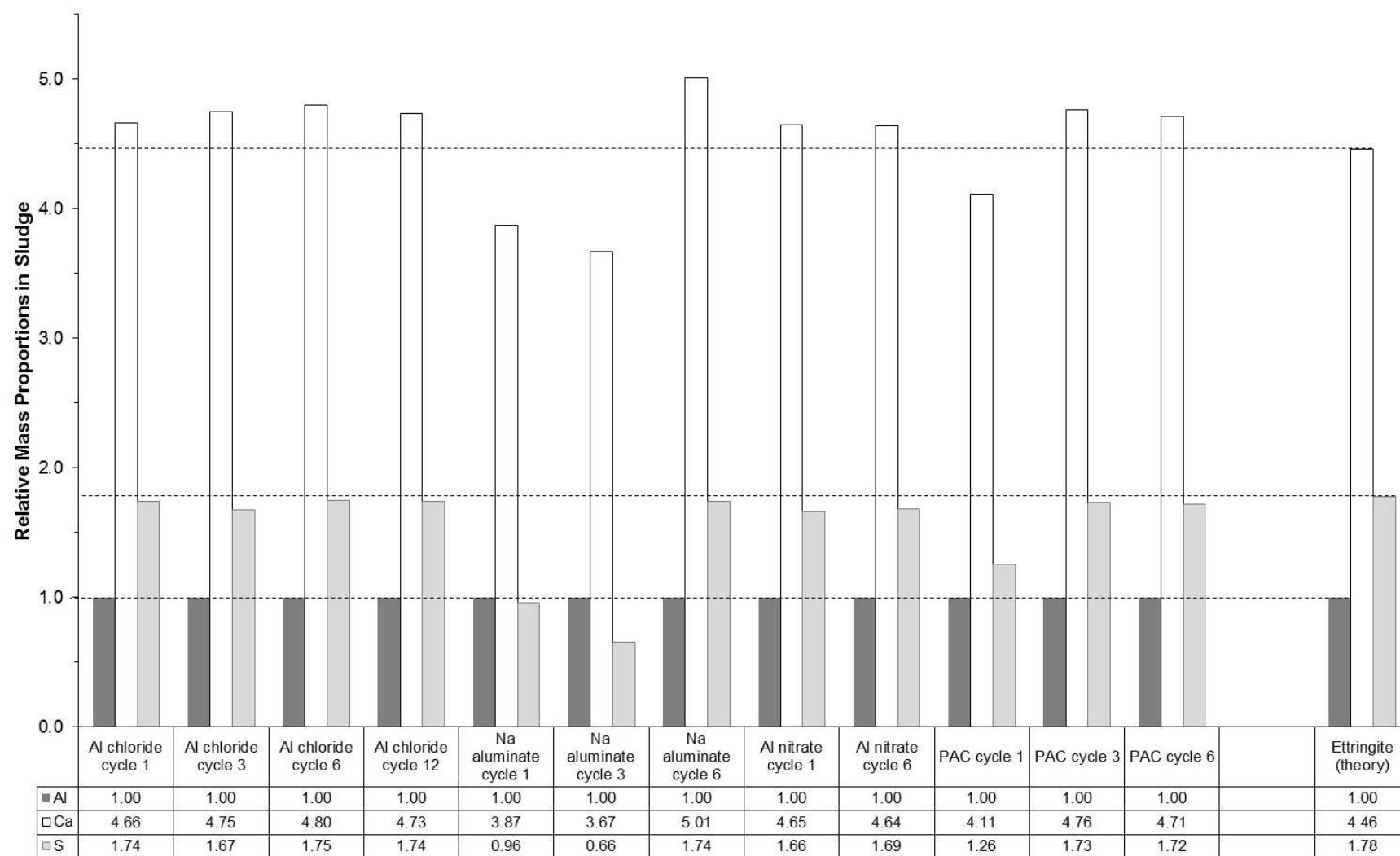
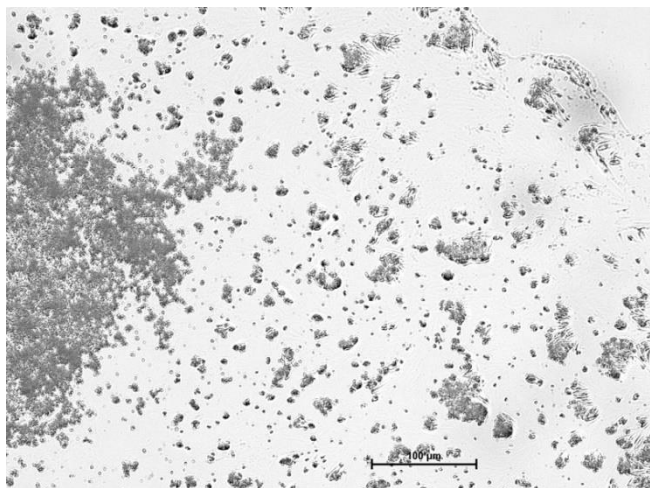
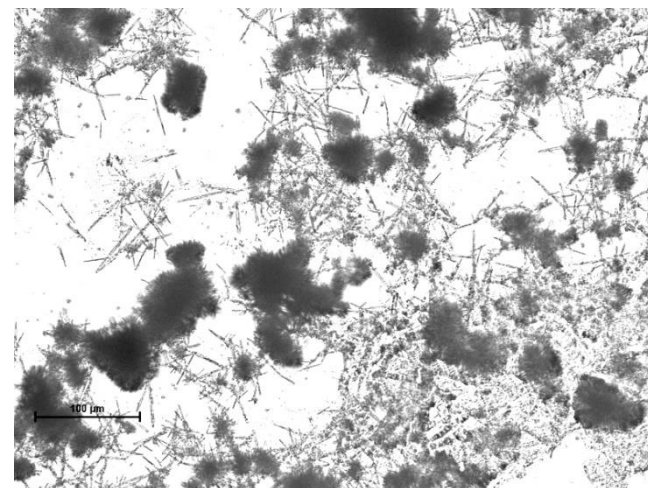


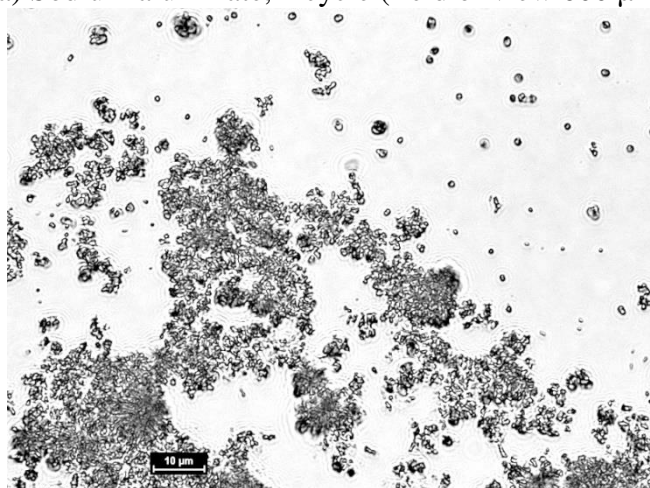
Fig 6. Ratios of Al, Ca, S in precipitates normalised to unit Al



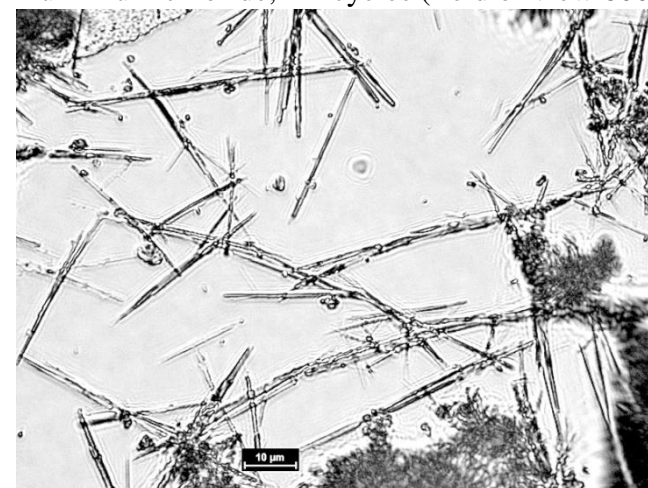
(a) Sodium aluminate, 1 cycle (field of view 600 μm)



(b) Aluminium chloride, 12 cycles (field of view 600 μm)



(c) Sodium aluminate, 3 cycles (field of view 130 μm)



(d) Aluminium nitrate, 6 cycles (field of view 130 μm)

Fig. 7 Microscope images of precipitates formed from reagents as indicated, highlighting differences in morphology, c.f. descriptions in Table 2

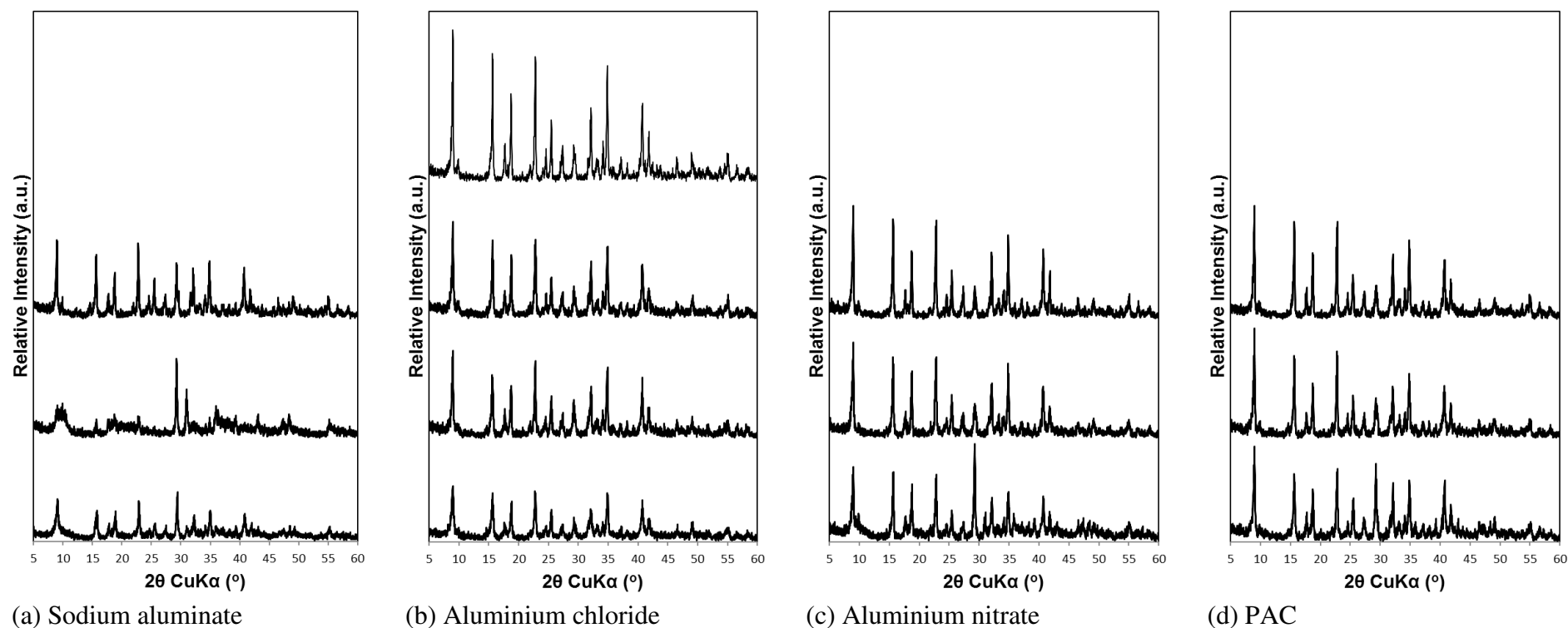


Fig 8. XRD spectra for precipitates for cycles 1, 3, 6 and 12 (for aluminium chloride) from bottom upwards.

Tab 2. Microscopy observations of precipitate morphology

Aluminiferous Reagent	Cycle Number	Observation
Sodium aluminate	1	Clusters of small spheres ~ 1µm
	3	Clusters of small spheres ~ 1µm
	6	Clusters of small spheres ~ 1 - 5 µm. Occasional small needles ≤ 10 µm
Aluminium chloride	1	Clusters of small spheres ~ 1µm. Occasional small needles ≤ 10 µm
	3	Mixture of clumps with radiating edges, small spheres ~ 1µm and free needles ≤ 10 µm
	6	Mixture of clumps with radiating edges, small spheres ~ 1µm and free needles ≤ 10 µm
	12	Mixture of clumps with radiating edges, small spheres ~ 1µm and long free needles ~ 50 µm
Aluminium nitrate	1	Clusters of small spheres ~ 1 - 5 µm. Rare small needles ≤ 10 µm
	6	Mixture of clumps with radiating edges, small spheres ~ 1µm and long free needles ~ 50 µm
PAC	1	Clusters of small spheres ~ 1µm
	3	Clusters of small spheres ~ 1µm. Occasional small needles ≤ 10 µm
	6	Mixture of clumps with radiating edges, small spheres ~ 1µm and long free needles ~ 50 µm

As the chemical environment, including both the reagent used (as shown in this paper) and other species present (other studies outline above) appears to play such an important role in determining the nature of the precipitate that forms, these effects must be evaluated for the process feed.

4. Conclusions

The experiments show that aluminum chloride (AlCl_3), aluminum nitrate ($\text{Al}_2(\text{NO}_3)_3$) and polyaluminum chloride (PAC) all form ettringite and remove sulfate, with AlCl_3 giving the best results over a single reaction cycle. Powdered crystalline gibbsite and laboratory synthesised $\text{Al}(\text{OH})_3$ were found not to form ettringite. Sodium aluminate (NaAlO_2) resulted in a precipitate with a chemistry deviating from that of ettringite and the other precipitates, possibly indicating formation of a mixed ettringite calcium aluminate monosulfate phase and also displayed different XRD spectra for 1–3 cycles. Upon recycling the sodium aluminate-derived sludge took longer to evolve needle-like crystals than the other reacting systems, although by the 6th cycle the XRD spectra and compositional analyses indicated that the composition had evolved to be in line with the precipitates using the other reagents.

Of the aluminiferous reagents used, aluminum chloride gave the most promising performance for sulfate removal as ettringite because it produced the lowest volume sludge and lowest residual sulfate concentrations, the highest bound sulfate, and the fastest sludge settling velocities. Sodium aluminate was the least promising giving a much more voluminous, slow settling sludge, with lower bound sulfate. The performance of PAC and $\text{Al}(\text{NO}_3)_3$ derived sludge displayed properties between these.

Recycling of sludge in the process seemingly improves the precipitation kinetics, as indicated by lower residual sulfate concentrations found for the same reaction time upon sludge recycling. It is possible to densify the ettringite sludge through recycling of the

sludge in the process, although the effect is small. For aluminum chloride, aluminum nitrate or PAC, the optimum number of cycles was <8 cycles. This work serves to sound a precautionary note for industrial application of the ettringite process. Given the sensitivity of the sludge properties to the chemical environment in which the precipitates form, the chemistry of the effluent treated in addition to the aluminiferous reagent used may exert significant influence on the effectiveness and practicality of application of the final process. Thus establishing the link between reagents used, effluent chemistry and their effects on micro and macroscopic properties of the resultant ettringite sludge is an important area for future research. It is recommended that these effects are evaluated for the process feed whenever ettringite precipitation is proposed as a method for sulfate removal.

References

- [1] M.V. Galiana-Alexiandre, A. Iborra-Clar, B. Bes-Pia, J.A. Mendoza-Roca, B. Cuartas-Urbe, M.I. Iborra-Clar, Nanofiltration for sulphate removal and water reuse of the pickling and tanning processes in a tannery, *Desalination* 179 (1-3) (2005) 307–313.
- [2] R. Silva, L. Cadorin, J. Rubio, Sulphate ions removal from an aqueous solution: I. Co-precipitation with hydrolysed aluminum-bearing salts, *Miner. Eng.* 23 (15)(2010) 1220–1226.
- [3] S. Tait, W.P. Clarke, J. Keller, D.J. Batstone, Removal of sulfate from high-strength wastewater by crystallisation, *Water Res.* 43 (3) (2009) 762–772.
- [4] World Health Organization, Guidelines for Drinking-water Quality, 4th ed., WHO publications, 2011.
- [5] H.A.F. Dehwah, M.S. Maslehuddin, A. Austin, Long-term Effect of Sulfate Ions and Associated Cation Type on Chloride-induced Reinforcement Corrosion in Portland Cement Concretes, (2002).
- [6] Lorax, Treatment of Sulphate in Mine Effluent, International Network for Acid Prevention, 2003.
- [7] R.J. Bowell, A review of sulfate removal options for mine waters, *Proceed. Mine Water* (2004) 75–88.
- [8] M.A. Reinsel, A new process for sulfate removal from industrial waters, *Proceedings of the 16th Annual American Society for Surface Mining and Reclamation*, Scottsdale, AZ, Aug, 13–19, 1999.
- [9] D.J. Bosman, J.A. Clayton, J.P. Maree, C.J.L. Adlem, Removal of sulphate from mine water using barium sulphide, *Int. J. Mine Water* 9 (1-4) (1990) 149–163.
- [10] C. Adlem, J.P. Maree, P. du Plessis, Treatment of sulphate-rich mining effluents with the barium hydroxide process and recovery of valuable by-products, *Proc. 4th International Mine Water Assoc. Congress* (1991) 25–30.
- [11] W. Changqiu, M. Shengfeng, L. Anhuai, Z. Jiangong, Experimental study on formation conditions of ammoniojarosite and its environmental significance, *Acta Geol. Sin. (English Ed.)* 80 (2) (2006) 296–301.
- [12] J.K. Tishmack, P.E. Burns, Chemistry and mineralogy of coal, in: R. Gieré, P. Stille (Eds.), *Energy Waste and the Environment: a Geochemical Perspective*, The Geological Society Special publication 236, London, 2004pp. 223–246.
- [13] R.E. Damons, F.W. Petersen, An aspen model for the treatment of acid mine water, *Eur. J. Miner. Proc. Environ. Protect.* 2 (2) (2002) 69–81.
- [14] C.A. Johnson, Cement stabilization of heavy-metal containing wastes, in: R. Gieré, P. Stille (Eds.), *Energy Waste and the Environment: a Geochemical Perspective*, The Geological Society Special publication 236, London, 2004pp. 596–606.
- [15] G. Zhen, X. Lu, X. Cheng, H. Chen, X. Yan, Y. Zhao, Hydration process of the aluminate 12CaO· 7Al₂O₃-assisted Portland cement-based solidification/stabilization of sewage sludge, *Constr. Build. Mater.* 30 (2012) 675–681.
- [16] A.M. Cody, H. Lee, R.D. Cody, P.G. Spry, The effects of chemical environment on the nucleation, growth, and stability of ettringite [Ca₃Al(OH)₆]₂(SO₄)₃·26H₂O, *Cem. Concr. Res.* 34 (5) (2004) 869–881
- [17] E. Janneck, M. Cook, C. Kunze, K. Sommer, L. Dinu, Ettringite precipitation vs. nano-Filtration for efficient sulphate removal from mine water, *IMWA Conference* (2012).
- [18] P.D. Kostenbader, G.F. Haines, High density sludge treats acid mine water, *Coal Age* 75 (9) (1970) 90.
- [19] D.J. Bosman, The improved densification of sludge from neutralized acid mine drainage, *J. S. Afr. Inst. Min. Metall.* 74 (9) (1974) 340–348.

Sapsford, D.J. and Tufvesson, S., 2017. Properties of recycled sludge formed from different aluminiferous reagents during the ettringite process. *Journal of Water Process Engineering*, 19, pp.305-311.

[20] R.H. Coulton, C.J. Bullen, C.R. Williams, K.P. Williams, The formation of high density sludge from mine waters with low iron concentrations, *Proceedi. IMWA 2004* (2004) 25–30.

[21] D.J. Bosman, Lime treatment of acid mine water and associated solids/liquid separation, *Water Sci. Technol.* 15 (2) (1983) 71–84.

[22] M. Chrysochoou, D. Dermatas, Evaluation of ettringite and hydrocalumite formation for heavy metal immobilization: literature review and experimental study, *J. Hazard. Mater.* 136 (1) (2006) 20–33.

[23] M. Zhang, E.J. Reardon, Removal of B, Cr, Mo, and Se from wastewater by incorporation into hydrocalumite and ettringite, *Environ. Sci. Technol.* 37 (13) (2003) 2947–2952.

[24] H.F.W. Taylor, Crystal structures of some double hydroxide minerals, *Mineral. Mag.* 39 (304) (1973) 377–389.

[25] P.J. Usinowicz, B.F. Monzyk, L. Carlton, Technical and economic evaluation and selection of sulfate ion removal technologies for recovery of water from mineral concentrate transport slurry, *Proc. of the Water. Environ. Federation 2006* (13) (2006) 139–153.

[26] G. Madzivire, L.F. Petrik, W.M. Gitari, T.V. Ojumu, G. Balfour, Application of coal fly ash to circumneutral mine waters for the removal of sulphates as gypsum and ettringite, *Miner. Eng.* 23 (3) (2010) 252–257.

[27] W. Dou, Z. Zhou, L.M. Jiang, A. Jiang, R. Huang, X. Tian, W. Zhang, D. Chen, Sulfate removal from wastewater using ettringite precipitation: Magnesium ion inhibition and process optimization, *J. Environ. Manage.* 196 (2017) 518–526.